Published in final edited form as:
Brain Res. 2008 June 12; 1214: 145–158.

Multiple Expression of Matrix Metalloproteinases in Murine Neurocysticercosis: Implications for Leukocyte Migration Through Multiple Central Nervous System Barriers

Jorge I. Alvarez[1,2] and **Judy M. Teale**[1,2]

1 *Department of Microbiology and Immunology, University of Texas Health Science Center at San Antonio. 7703 Floyd Curl dr, San Antonio, TX 78229*

2 *Department of Biology, University of Texas at San Antonio. One UTSA circle, San Antonio, TX 78249*

Abstract

During the course of murine neurocysticercosis (NCC), disruption of the unique protective barriers in the central nervous system (CNS) is evidenced by extravasation of leukocytes. This process varies according to the anatomical sites and diverse vascular beds analyzed. To examine mechanisms involved in the observed differences, the expression and activity of eight matrix metalloproteinases (MMPs) were analyzed in a murine model of NCC. The mRNA expression of the MMPs studied was upregulated as a result of infection, and active MMPs were mainly detected in leukocytes migrating into the brain. Polarized expression and gelatinolytic activity of several MMPs were identified in immune cells extravasating pial vessels as early as 1 day post infection. In contrast, leukocytes expressing active MMPs and extravasating parenchymal vessels were not observed until 5 weeks post infection. In ventricular areas, most of the MMP activity was detected in leukocytes traversing the ependyma from leptomeningeal infiltrates. In addition, immune cells continued to express active MMPs after exiting vessels suggesting that enzymatic activity of MMPs is not just required for diapedesis. These results correlate with our previous studies showing differential kinetics in the disruption of the CNS barriers upon infection and help document the important role of MMPs during leukocyte infiltration and inflammation.

Keywords

neurocysticercosis; matrix metalloproteinases; blood brain barrier; blood cerebrospinal-fluid barrier; ventricle; ependyma

1. INTRODUCTION

Neurocysticercosis (NCC), a parasitic disease of the CNS is accompanied by disruption of the BBB that can lead to significant morbidity and mortality [61]. Our studies in a mouse model of NCC have revealed differential breakdown of the BBB and the blood-cerebrospinal fluid barrier (BCB) dependant upon the vascular bed, accumulation of blood derived leukocytes,

Corresponding author: Judy M. Teale, One UTSA circle, San Antonio, TX 78249, Phone: +1 210 4587024, Fax: +1 210 4587025, E-mail: judy.teale@utsa.edu.

production of inflammatory cytokines and differential expression of MMP-9 [2–4]. Many of these pathophysiological conditions have been described in other CNS disorders, and MMPs have been linked to associated mechanisms [28,43,63].

MMPs are an expanding family of endopeptidases that serve as effectors of cell migration, cytotoxicity and tissue remodeling via degradation of extracellular matrix (ECM) components [40]. MMPs are highly regulated in their expression, secretion and activity [29]. Generally, they are expressed at low or undetectable levels; however, expression is rapidly induced at times of active tissue remodeling. Neutrophils, macrophages, glial cells, vascular smooth cells, and T cells among others are able to produce MMPs upon stimulation [28]. MMPs are commonly transcribed and secreted by the constitutive secretory pathway, except in the case of immune cells such as neutrophils and macrophages where they are stored in secretory granules and released upon stimulation [32]. MMPs are secreted in response to exogenous insults and inflammatory cytokines such as TNF-α [10] and IL-1β [56]. Additionally, cell contact dependent signaling may drive MMP up-regulation [27,37]. MMP secretion is down-regulated by diverse cytokines including IFNγ, IL-4 and IL-10 [16,36,60], although the regulation of secretion is cell- and stimulus-specific. Upon infection the challenged host immune system must recruit leukocytes to the site of infection, eliminate the pathogen and then downregulate the response to allow resolution of the inflammatory process. MMPs play an important role in these processes both by degrading components of the ECM and by modulating cytokine and chemokine activity [19].

In the normal adult CNS, most MMPs are expressed at intermediate to low levels. RNase protection and polymerase chain reaction assays have shown constitutive expression of MMP-2, -3, - 7, -8, -9, -11, -13, -14, -15, -16, -17, -19, -20, -21 and -23 in rodents [15,54,58]. In normal rat brain, MMP-2 expression has been described in astrocyte endfeet [45]. Upregulation of MMPs has been reported in multiple sclerosis, stroke, HIV-dementia, bacterial meningitis, Alzheimer's disease and brain tumors [43,46,47,63]. Animal models used to study distinct CNS disorders have concentrated on the use of MMP inhibitors or MMP deficient animals to evaluate the lack of MMPs in the progression of the disorder [7,24,28,29,35,43]. Studies in humans have focused on detection of MMPs in serum, CSF or post-mortem specimens, and in general the data obtained correlates positively with the severity of the disorder [5,14,22,26,33,48]. However, measurement of MMP expression and activity has rarely been evaluated in vivo. In addition, changes in BBB and BCB permeability associated with MMP expression have not addressed the different vascular beds or the complex anatomy of the CNS.

Thus, the aim of this study was to evaluate the mRNA and protein expression of MMPs in mice infected with *Mesocestoides corti* which is closely related to *Taenia solium*, the cestode that causes NCC in humans. Particular emphasis was given to the expression of MMPs in leukocytes extravasating different types of vasculature as the kinetics of infiltration differs among distinct areas of the mouse brain [2–4]. Total mRNA isolated from brains after different post infection times was analyzed using a macroarray specific for MMPs. In situ zymography and immunofluorescence microscopy were performed in brain cryosections to analyze the active expression of MMPs in leukocytes invading the CNS. A wide variety of MMPs are upregulated upon infection, and most of the activity of these enzymes was detected in leukocytes invading the CNS through leptomeninges, parenchyma and ventricles. In addition, the extent and timing of MMP activation differ among pial, parenchymal and ventricular vessels. The findings suggest that differential activation of multiple leukocyte MMPs is required to support the anatomical heterogeneity of immune cell extravasation and migration in infected brain.

2. RESULTS

MMP specific RNA is upregulated in parasite infected brain

As an initial screen to determine if MMPs are upregulated in a murine model of NCC, brain levels for a number of MMP specific RNAs were compared with mock infected controls. Macroarray analysis of samples obtained from mock infected animals showed relatively low levels of mRNA for most of the MMPs analyzed except for MMP16 (MT3-MMP) and TIMP-2 (Fig 1). Upregulation of MMP mRNAs during the infectious process was observed for most of the MMPs analyzed (Fig 1). It was generally characterized by a maximum level of expression at 1 wk of infection followed by downregulation at 3 and 5 wk (Fig 1), except for MMP-8 and -9 which exhibited maximum expression at 3 wk (Fig 1). MMP-2 and -3 were only slightly upregulated (Fig 1) but have been described in the pathogenesis of other CNS disorders [23, 63].

Leukocytes express active MMPs in a polarized fashion when exiting pial vessels early in the infection

During the course of murine NCC, leukocytes first extravasate through pial vessels located in the external and internal leptomeninges [2]. MMP-9 expression and activity has been demonstrated in this process [4], but upregulation of multiple MMPs upon infection (Fig 1) may indicate that simultaneous activity of different MMPs is necessary to support leukocyte extravasation into the CNS. To test this hypothesis we studied both the expression and potential enzymatic activity of distinct MMPs in leukocytes exiting pial vessels of mock and parasite infected animals. In mock infected control animals, relatively little expression and gelatinolysis activity were found in the few leukocytes detected after multiple sections were analyzed (Table 1 and Fig 3). An example of MMP-2 is shown in Fig 2A to 2C. In contrast, collagenolysis activity in leukocytes was mostly undetectable in these animals (Table 1). This is consistent with our previous studies in which few leukocytes could be found infiltrating into the CNS of control or mock infected animals [2,4]. It is probable that some degree of MMP activity in the form of gelatinolytic activity is required for leukocytes extravasating into the CNS under normal physiological conditions.

Leukocytes traversing pial vessels of animals infected for 1 and 3 days exhibited upregulation of multiple MMPs with most of the enzymatic activity associated with gelatinolysis (Table 1 and Fig 3). Importantly, the gelatinolytic activity of leukocytes exiting pial vessels was polarized from the lumen of the vessel towards the nervous tissue strongly suggesting its role in directionality of cell movement. MMP-2 (Fig 2D to 2F), -9 (Fig 2G to 2I), and -8 (Fig 2J to 2L) were most evident in this polarized pattern of both expression and gelatinolytic activity. MMP-7 expression was hardly detected in early infiltrating cells, but it was highly upregulated in pial vessels although the potential substrate remains undefined (Fig 2M to 2O). In infected animals, polarized activity of MMPs was less evident when collagen was used as the substrate for ISZ. In addition, collagenolysis in general was found at lower levels than gelatinolysis in cells infiltrating the brain at days 1 and 3 post infection (Table 1).

Active MMPs continue to be expressed in leptomeningeal inflammatory infiltrates

From our previous studies, immune cells continue to accumulate in the internal and external leptomeninges for several weeks [2,12], so MMP expression and activity was studied at later post infection times in these areas. At 1, 3 and 5 wk post infection; the expression and apparent activity of multiple MMPs were present in infiltrates using either substrate although to varying degrees (Table I, Fig 3). Examples of specific MMPs at different time points using gelatin or collagen are shown in Figs 4 and 5 respectively. Leukocyte infiltration and expression of active MMPs increased after 1 wk of infection (Table 1,Fig 4A–C). An antibody to CD11b which detects myeloid cells was also used in conjunction with ISZ using gelatin as substrate (Fig 4D–

F). The results indicate a large portion of the cells extravasating pial vessels and exhibiting gelatinolytic activity are macrophages. In murine NCC there is a moderate infiltration of neutrophils [2], MMP-9, -8, -3, -2 and -12 were also detected in cells displaying neutrophil-like morphology. At the later post infection times of 3 and 5 wks, there were increased amounts of infiltrates surrounding vessels and accumulating in leptomeninges (Figs 4G–O, Fig 5D–L). Importantly, the majority of cells present in large infiltrates continue to exhibit MMP activity indicative of their role in both diapedesis and migration through the ECM. This was particularly evident for MMP-8 (Fig 4M–O, Fig 5D–F) and MMP-16 (Fig 5D–F). Also evident at the later time points was an increase in collagen cleavage compared to earlier time points.

Upregulation of MMP-7 in pial vessels with unknown substrate activity was also found at later times post infection (Fig 4J–L). In addition, MMP-3 was expressed in pial vessels (Fig 4G) and moderate gelatin degradation was observed (Fig 4G–I). Also of interest, astrocyte endfeet opposing the pia had increased expression of some MMPs although they were inactive in terms of gelatin and collagen cleavage. Increased expression in astrocyte endfeet was most pronounced with MMP-2 (Figs 4A–4C), -3, -8 (Figs 4M, 4O and 5J), -9, -12 (Figs 5A–5C), -13 (Figs 5G–5I) and -16.

Leukocytes infiltrating through parenchymal vessels express active MMPs

Unlike pial vessels in leptomeninges that display leukocyte infiltration by day 1 of infection, in recent studies we have shown that leukocytes exiting parenchymal vessels do not occur until 5 wks after infection [2]. In addition, we showed that MMP-9 is an important player in this process using MMP9 $^{-/-}$ mice [4]. To further understand the role of MMPs in the breakdown of parenchymal vessels, the expression and potential enzymatic activity of additional MMPs were studied. Extravasation of serum proteins such as fibronectin has been used as a marker of BBB disruption [2,38,39]. To correlate BBB disruption with MMP activity, cleavage of gelatin and fibronectin leakage were studied simultaneously in parenchymal vessels at distinct post infection times. It was found that overt leakage of fibronectin correlates with MMP activity, but neither were detected in parenchyma until the fifth week of infection (Fig 6A to 6C)[2]. Examples of leukocytes expressing MMP-2 and MMP-8 with gelatinolytic activity are shown in Fig 6D-F and Fig 6G-I respectively, and examples of MMP-13 and MMP-16 with collagenolytic activity in Fig 6J–L and Fig 6M–O. Similar to observations in pial vessels of the leptomeninges, a relatively large proportion of cellular infiltrates expressed MMP-8 and MMP-16 with colocalized enzymatic activity. Moreover, there was no evidence for a distinct pattern of MMP expression or activity that could explain differences in the timing of leukocyte infiltration when comparing parenchymal and pial vessels.

Differences in the expression of certain MMPs were detected in the astrocyte endfeet ensheathing parenchymal vessels vs. those opposing the pia. After 1 wk of infection and at later post-infection times, substantial expression of various MMPs, as described above, were detected in astrocyte endfeet opposing the pia. Those in vicinity of parenchymal vessels only expressed detectable levels of MMP-2 (Fig 6D). However, the MMPs expressed by these two different populations of astrocytes were inactive in terms of gelatin and collagen cleavage.

Active MMPs are expressed in leukocytes infiltrating ventricular areas

Leukocytes can access the CNS by entry into ventricles through the choroid plexuses (CPs). In fact, this is the normal entry point in the uninfected brain. We have recently shown that leukocytes predominately access the ventricles during infection by disruption of pial vessels in the subependymal area followed by migration of leukocytes into ventricles through a compromised ependymal lining, the epithelial layer that surrounds the ventricle [3]. Therefore, we evaluated the expression and activity of MMPs to assess their involvement in leukocyte migration into ventricles. Among the MMPs expressed in the ependyma of mock infected

animals, MMP-8 (Fig 7A) and MMP-3 showed a higher expression, but these MMPs were mostly inactive in control animals (Fig 7A). Relatively low levels of inactive MMP-2, -9, -12 and -16 were also detected in ependyma, whereas no expression of MMP-7 and -13 was observed (Table 1).

Infected animals exhibited scarce activity of MMP-8 and MMP-3 at days 1 and 3 of infection (data not shown). Expression of MMP-2, -9, -12 and -16 was similar to mock infected controls. By 1 wk of infection, there was an increase of infiltrates in the subependyma exhibiting gelatinolyitc and collagenolytic activity (Fig 7B–E). Some of these infiltrating cells colocalized with MMPs and examples of MMP-8, -12, -16, and -9 are shown in Fig 7B–E, respectively. Later post infection times of 3–5 wks showed increasing numbers of leukocytes expressing active MMPs (Table 1). Consistent with our previous results indicating infection-induced breaks in the ependyma as a source of inflammatory infiltrates in ventricles[3], Fig 7F shows large numbers of $CD11b^+$ cells (presumably macrophages) that have appeared to cross through the ependymal lining (demarcated by cadherin staining) into the ventricle. Also shown is the active expression of MMP-12 (Fig 7G), MMP-8 (Fig 7H), and MMP-2 (Fig 7I).

Leukocyte extravasation through the CPs is relatively low during murine NCC [2,3]. Of the cells that appear to be exiting the CPs, expression of MMP-12 (Fig 7C) and MMP-16 was found mainly exhibiting collagen activity, and to a lesser extent MMP-3 exhibiting gelatin cleavage. Finally, the presence of MMP-2 and -9 noted above in the astrocyte endfeet opposing the pia were also upregulated in the astrocyte endfeet in contact with ependyma. However, in contrast to the lack of activity next to the pia and parenchymal vessels, gelatin cleavage was detected in periventricular areas as shown in Fig 7E and Fig 7I.

3. DISCUSSION

MMP function has been classically associated with remodeling of the ECM, but their role in leukocyte recruitment and processing of cytokines, chemokines, defensins and adhesion molecules is increasingly apparent [19,63]. These multifunctional capabilities suggest that several members of this family are involved in the inflammatory process, and our results showing upregulation of multiple MMPs at the RNA level support this hypothesis albeit distinguishing between pro- and active MMPs is essential. Infiltrating leukocytes have been shown to be a major source of MMPs in distinct CNS disorders [21,25,31,55,59]. However, studies in this area have generally focused on a particular MMP and enzymatic activity, mostly cleavage of gelatin. In this study, the activity of multiple MMPs was assessed at various times post infection by both gelatin and collagen cleavage using ISZ so that MMP expression and activity could be studied at the single cell level. Increased expression of several MMPs was noted in astrocytic endfeet in proximity to areas of inflammation as discussed below. However, the vast majority of increased expression and activity of the 8 MMPs analyzed here were associated with infiltrating immune cells. Although CD11b was the only cell surface marker shown, we know from our previous studies that multiple cell types are present in the infiltrates [2,12], and many CD11b negative cells are expressing active MMPs. Therefore CD11b positive cells, presumably macrophages/microglia, are an important source of MMPs, but it is likely that all immune cells that exit CNS vessels express MMPs in order to extravasate.

Also lacking in previous studies is the location of inflammatory infiltrates as it relates to MMP expression, and this is critical given the complex anatomy and distinct barrier functions associated with different types of brain vasculature. We recently found that in murine NCC, BBB disruption and leukocyte migration occurs through pial vessels within days but in parenchymal vessels, it takes up to 5 weeks [2]. In the study shown here, we found expression of multiple, enzymatically active MMPs within the population of leukocytes extravasating pial vessels as early as 1 day after infection. These findings suggest that leukocytes extravasating

early in the infection require activity of multiple MMPs to migrate through the junctional complex proteins of pial vessels and through the complexity of molecules associated with the basal lamina normally present to protect the brain in the absence of disease. Importantly, many of the MMPs analyzed in this study i.e: MMP-2, -3, -7 and -9, are known to degrade junctional complex proteins such as occludin, claudin-5, ZO1 and VE-cadherin [6,13,62]. MMP-8, -16 and those previously named were actively expressed by leukocytes and pial vessels, indicating a correlation with our previous results of the timing of BBB disruption and the discontinuous expression of junctional complex proteins in CNS vessels [2,4]. It is also possible that distinct subsets of leukocytes differ in the predominant MMPs utilized for extravasation.

Interestingly, the enzymatic activity of MMPs detected at these very early time points involved gelatin degradation more so than collagen activity. At these early time points, the main event being analyzed is likely the diapedesis process as opposed to migration through the leptomeninges. Thus, it appears that gelatinolytic activity is more important for exiting the vessel itself. This is consistent with the more polarized activity associated with gelatin degradation compared with collagen. As the infection ensues, there is a progressive accumulation of infiltrating leukocytes in the leptomeninges, and enzymatic activity of multiple MMPs for both gelatin and collagen degradation is apparent. Movement of leukocytes within the perivascular and Virchow-Robin spaces requires active MMPs to remodel the ECM in these areas which is a hyaluronate-rich matrix composed of proteoglycans (e.g. neurocan, aggrecan), glycoproteins (e.g. laminin and fibronectin), and numerous others factors such as agrin and polysialic acid [11,42]. In addition, direct contact between leukocytes accumulated in these infiltrates can induce additional expression of MMPs [17]. Moreover, MMPs also modulate the expression and secretion of cytokines and chemokines that promote or restrict further leukocyte extravasation and immune cell interaction in inflammatory infiltrates [19, 30,34]. As the immune infiltrates found during the course of murine NCC are composed of a heterogeneous population of immune cells including macrophages, γδ T cells, αβ T cells, neutrophils, and B cells [2,12], mechanisms that upregulate or downregulate the overall immune response via cleavage of cytokine, chemokine and adhesion molecules could be accomplished by the multiple expression of MMPs. Thus, enhanced expression of various MMPs in inflammatory infiltrates of animals infected with *M. corti* likely sustains accumulation of additional leukocytes by facilitating further extravasation through vasculature as well as through the ECM. In particular, the high expression and activity of MMP-8 in this model contrasts reports from most of the findings in other CNS disorders where MMP-2, -3 and -9 appear to be the main players in the pathological process [1,21,28,62,63]. In murine NCC, MMP-8 cleaved both gelatin and collagen, and it was detected in most of the areas analyzed, indicating its crucial role during the course of this infectious disease.

Leukocyte infiltration in parenchyma is a process directly associated with the kinetics of BBB disruption, which is generally delayed during neuroinflammation compared with leptomeninges [2,41]. Expression of active MMP-9 in parenchymal vessels correlates with the timing of leukocyte infiltration, but its absence does not completely abrogate this process [4]. In the present study, expression of other MMPs was not detected around parenchymal vessels until the fifth week of infection providing a direct correlation with the timing of leukocyte infiltration and with the changes in expression of junctional complex proteins in this type of vasculature that we reported previously [2,4]. Differential kinetics of leukocyte infiltration between pial and parenchymal vessels may be explained in part by the distinct pattern of adhesion molecules and extent of endothelium activation that have been described in these two types of vessels [9,41]. Also, additional barriers in the parenchyma provide a likely explanation of why immune cell infiltration through parenchymal vessels is delayed and why expression of multiple MMPs may be a requirement. Leukocytes that have moved through parenchymal vessels first cross the endothelial basal lamina but then need to traverse the parenchymal basement membrane followed by membranes of the astrocytic endfeet processes. Pial vessels

are not ensheathed by astrocytes nor do they have a parenchymal basement membrane. The parenchymal basement membrane contains laminins, α1 and α2, compared with the endothelial basal lamina that only contains laminin α4 [49,57] suggesting a more complex barrier. Additionally, the parenchymal basement membrane is linked to the astrocytic endfoot membrane through interactions with ECM components present on both sides [51,52]. Dystroglycan, which is exclusively expressed on the astrocytic endfoot membrane [53,64] participates in these interactions, and it is known to be a substrate of MMP-2 and -9 [1]. In light of these findings, the delay in leukocyte extravasation is likely the result of increased barriers that serve to protect endothelial cells of parenchymal vessels of the necessary signals for leukocyte diapedesis which includes activation of functional MMPs. However, the leukocytes that exit and accumulate outside of pial and parenchymal vessels display the same multiple MMPs with both gelatinolytic and collagenolytic activity. Although the determination of specific substrates will be crucial, no evidence was found indicating that the differential kinetics of leukocyte infiltration between pial and parenchymal vessels was the result of a particular MMP exhibiting gelatinolytic or collagenolytic activity.

In murine NCC, leukocytes infiltrating ventricular spaces mainly come from pial vessels of the subependyma and to a lesser amount, migrate through the CPs [2,3]. In this report, the activity of multiple MMPs was studied in the ependyma, choroid plexus and leukocytes infiltrating these areas. Immune cells coming from subependymal pial vessels expressed multiple active MMPs using both substrates when they were sub-adjacent to the ependyma or traversing it. The composition of the subependyma basal lamina opposing leptomeninges remains to be fully investigated, but in contrast with the pial vessel basal lamina, hyaluronic acid is not detected [8]. In addition, in normal mice the expression of tight junction proteins such as claudin-1, -3 and -5 is not detected in ependyma [3] indicating that the barrier properties of this structure are less restrictive compared with CNS vessels. Moreover, the junctional complex proteins expressed in ependyma appear discontinuous or undetectable during infection [3]. Expression of MMP-2, -3, -8 and 12 in the ependyma of infected animals was upregulated compared with mock infected animals suggesting that this epithelium may be able to support leukocyte migration by activating chemokines and/or adhesion molecules during infection. Taken together, the ependyma located in proximity to leptomeninges and its basal lamina appear to be less restrictive for cell migration due to the unique expression of MMPs in this epithelium, to the high expression of active MMPs in inflammatory leukocytes and to its less intricate junctional complexity and ECM composition.

In contrast to the multiple MMPs found in ependymal cells and leukocytes moving through this cellular layer, the choroid plexus and the cells extravasating it showed a more limited expression of MMPs. Moderate upregulation in the expression of MMP-3, -12, and -8 and low enzymatic activity was detected by ISZ. These findings complement a recent report showing the lack of structural changes in junctional complexes of the CPs of animals infected with *M. corti* [3]. These results are consistent with previous observations in an in vitro model showing that exposure to pro-inflammatory cytokines increased MMP-9 secretion by the choroidal epithelium and led to functional differences in permeability but not structural changes of the junctional complexes [50] although the permeability changes in this model may have been more notable. The ability to maintain the integrity of junctional complex proteins together with the more limited activity of MMPs in the CPs helps to explain why the CPs are a limited source of inflammatory cells in the CNS during infection.

Previous studies have shown that MMP action upon CNS injury is due to intrinsic expression and activation of astrocytes and microglia [20,44]. As mentioned above, upregulation of MMP expression was mainly found in infiltrates but was also noted in astrocytic endfeet adjacent to areas of inflammation. Interestingly, as a result of infection astrocytic endfeet that comprise the glia limitans adjacent to the pia and leptomeninges exhibit upregulation of most of the

MMPs analyzed, and they were inactive in terms of gelatin and collagen cleavage. The astrocytic endfeet opposing the ependyma also display increase expression of various MMPs, but with active gelatin cleavage in the case of MMP-2 and MMP-9. Both of these sites of inflammation are characterized by more permissive areas of cellular infiltration upon infection. In contrast, the astrocytic endfeet or glia limitans that surround parenchymal vessels, the least permissive environment for cellular migration, exhibited upregulation of mainly inactive MMP-2 and MMP-9. Therefore, astrocytes may also play an important role in barrier disruption during disease, an area that warrants further study.

Finally, this is the first study covering in situ, the multiple and active expression of various MMPs during a neuroinflammatory process. The assessment of all these enzymes in different areas of the CNS correlated with the changes in permeability and cellular infiltration in the various anatomical beds and vascular beds analyzed. The data suggest that multiples MMPs are required to support the complex nature of leukocyte infiltration and immunopathology observed in this model. Studies designed to block the activity of various MMPs and further define substrates will help to gain a better understanding of these processes.

4. EXPERIMENTAL PROCEDURE

Animals

Female BALB/c mice 3–5 wk old were purchased from the National Cancer Institute Animal Program (Bethesda, MD). Animal experiments were conducted under the guidelines of the University of Texas System, The U.S. Department of Agriculture, and the National Institutes of Health.

Parasites and inoculations

M. corti metacestodes were maintained by serial intraperitoneal inoculation of 8 to 12 wk old female BALB/c mice. Intracranial inoculations were performed as described previously [12]. For i.c. inoculations, parasites were aseptically collected from the peritoneal cavity and extensively washed in HBSS. Then, metacestodes (50 larvae) were suspended in 50 μl of HBSS and injected intracranially into 3–5-wk-old female mice using a 25-gauge needle [12,18]. The needle was inserted to a 2-mm depth at the junction of the superior sagittal and the transverse sutures. This allows insertion of the needle into a protective cuff avoiding penetration of the brain tissue. Control mice were injected with 50 μl sterile HBSS using the same protocol. Before intracranial inoculation, mice were anesthetized intramuscularly with 20 μl mouse mixture containing 100 mg/ml ketamine and 20 mg/ml rompum (Laboratory Animal Resource, University of Texas Health Science Center, and San Antonio, TX). Animals were sacrificed at 1 d, 3 d, 1 wk, 3 wk and 5 wk after inoculation and analyzed for parasite burden and immune cell infiltration. As previously reported, parasites were detected in meningeal, parenchymal and ventricular areas [2,3,12]. Before sacrifice, animals were anesthetized with 25 μl of mouse mixture and perfused through the left ventricle with 15 ml of cold PBS. Five or more animals were analyzed for each post-infection time with multiple sections analyzed per animal.

RNA isolation and gene array analysis

To determine the gene expression of MMPs during the course of infection, brains (n=2 per infection time) were immediately removed after perfusion and total RNA was extracted using Trizol (Invitrogen, Carlsbad CA) according to manufacturer's protocol. Levels of MMP mRNA were determined in the brain samples by using GEarray Q series mouse ECM and adhesion molecules gene array (SuperArray, Frederick MD) following manufacturer's instructions. Four micrograms of total RNA from each sample were reverse transcribed into cDNA in presence of α-^{33}P-dCTP using the templates and reverse transcriptase supplied in kits. The cDNA probes obtained were hybridized to gene specific cDNA fragments spotted on the GEArray

membranes. The specificity of the reaction was determined using the blank spots or those with cDNA fragments of the PUC18 plasmid. The radioactive signal from bound probes was measured using the Typhoon^{TM} 9400 phosphor imaging system (Molecular Dynamics, Sunnyvale CA). The numerical value corresponding to the intensity of the gene band was recorded and corrected for the background level of each blot using Image Quant software (Molecular Dynamics, Sunnyvale CA). The average intensity of each gene was normalized to the average values recorded for two housekeeping genes, cyclophilin A and rpI13a which were included in the blot for internal controls. The normalized value represented mRNA expression for each MMP gene.

Tissue processing and histological analysis

Brains removed from perfused animals were embedded in O.C.T. resin (Sakura, Torrance, CA) and snap frozen. Serial horizontal cryosections of 10 μm were placed on xylene prep slides (Sigma-Aldrich, St. Louis, MO). One in every five slides was stained with hematoxylin and eosin (H&E) to determine the location of parasites and cellular infiltrates. H&E slides were analyzed with a Leica DMR microscope (Leica Microsystems, Wetzlar Germany). Images were acquired using a cooled CCD SPOT RT camera (Diagnostic instruments Inc, Sterling Heights, MI). The images were processed and analyzed using Adobe Photoshop 7.0 (Adobe, Mountain View, CA). The remainder of the slides was air dried overnight and fixed in fresh acetone for 20 seconds at rt. Acetone-fixed sections were stored at −80°C or processed immediately for immunostaining.

Antibodies

Antibodies purchased from Triple Point Biologics (Forest Grove, OR) were all produced in rabbit and include anti-stromelysin-1 (MMP-3) carboxyterminal end, anti-matrilysin (MMP-7) animoterminal end of active MMP7, anti-macrophage elastase (MMP-12) carboxyterminal end, anti collagenase-3 (MMP-13) hinge region and anti-membrane-type MMP-3 (MT3-MMP, MMP-16) hinge region. Antibodies purchased from SIGMA (St Louis, MI) were also developed in rabbit and include anti-gelatinase A (MMP-2) hinge region, anti-collagenase 2 (MMP-8) hinge region and anti-gelatinase B (MMP-9). Rat anti-CD11b phycoerithrin(PE)-conjugated was purchased from BD PharMingen (San Diego, CA). The purified rabbit anti-fibronectin was purchased from Chemicon International (Temecula, CA). Finally the rabbit anti-pan-cadherin was purchased from Zymed laboratories (South San Francisco, CA). Anti MMP antibodies and fibronectin were detected with a RRX-conjugated AffiniPure donkey anti-rabbit IgG from Jackson ImmunoResearch (West Grove, PA). All antibodies were titrated with brain sections from 2 wk infected animals to determine optimal concentrations prior to use. Spleen and liver sections from animals intraperitoneally infected with *M. corti* were used as positive controls in titration experiments.

Immunofluorescence microscopy

Immunofluorescence (IF) staining was performed as previously described [2]. Briefly, tissues were fixed in −20°C acetone for 10 min and then hydrated in PBS. Non-specific immunoglobulin binding was blocked by 30 min incubation at rt with 10% serum from the same species that the fluorochrome conjugated antibodies were derived. Sections were incubated for 40 min with primary antibodies diluted in 3% species specific serum. Sections were washed 7X for 3 min each after incubation with specified antibodies. Secondary antibodies were incubated for 30 min at rt when necessary. Then, sections were mounted using fluorsave reagent (Calbiochem, La Jolla, CA) containing 0.3 μM 4',6'-diamidino-2-phenylindole dilactate-DAPI (Molecular Probes, Eugene, OR). Negative controls using secondary antibodies alone were included in each experiment and found to be negative for staining. Fluorescence was visualized in a Leica DMR epifluorescent microscope (Leica

Microsystems, Wetzlar Germany). Photographs were acquired, as described above. Imaging processing and analysis was done using Image Pro Plus 5.0 (Media Cybernetics, Silver Spring MD) and Adobe Photoshop 7.0 (Adobe, Mountain View, CA).

In situ zymography

In situ zymography (ISZ) was used to detect and localize gelatinolytic and collagenolytic activity in brain tissue. Sections that had been stored at −80°C were fixed and hydrated for IF analyses. A solution containing DQ-gelatin or collagen (Molecular probes, Eugene, OR), which are MMP substrates heavily labeled with fluorescein and Oregon 488 respectively, were used to determine activity of MMPs in situ. These substrates are heavily quenched and upon digestion the increase in fluorescence is proportional to MMP activity. Sections were incubated 40 min at rt with 1 μg/mL of DQ-gelatin in reaction buffer (0.05 M Tris-HCl, 0.15 M NaCl, 5 mM $CaCl_2$, pH 7.6) or with 5 mg/mL of collagen-oregon 488 in PBS 1X, and then washed. IF staining was analyzed to correlate the levels of active and inactive MMPs in the samples. Negative controls included pre-incubation with the MMP inhibitor 1, 10-phenanthroline (10 mM) and EDTA (10 mM). Images were acquired, processed and analyzed as previously described.

Acknowledgements

This work was supported by National Institutes of Health grants NS35974, AI 59703.

We thank Sandra Ojeda and Bibhuti Mishra for technical support.

References

1. Agrawal S, Anderson P, Durbeej M, van Rooijen N, Ivars F, Opdenakker G, Sorokin LM. Dystroglycan is selectively cleaved at the parenchymal basement membrane at sites of leukocyte extravasation in experimental autoimmune encephalomyelitis. J Exp Med 2006;203:1007–19. [PubMed: 16585265]
2. Alvarez JI, Teale JM. Breakdown of the blood brain barrier and blood-cerebrospinal fluid barrier is associated with differential leukocyte migration in distinct compartments of the CNS during the course of murine NCC. J Neuroimmunol 2006;173:45–55. [PubMed: 16406118]
3. Alvarez JI, Teale JM. Differential changes in junctional complex proteins suggest the ependymal lining as the main source of leukocyte infiltration into ventricles in murine neurocysticercosis. J Neuroimmunol 2007;187:102–13. [PubMed: 17597230]
4. Alvarez JI, Teale JM. Evidence for differential changes of junctional complex proteins in murine neurocysticercosis dependent upon CNS vasculature. Brain Res 2007;1169:98–111. [PubMed: 17686468]
5. Anthony DC, Ferguson B, Matyzak MK, Miller KM, Esiri MM, Perry VH. Differential matrix metalloproteinase expression in cases of multiple sclerosis and stroke. Neuropathol Appl Neurobiol 1997;23:406–15. [PubMed: 9364466]
6. Asahi M, Wang X, Mori T, Sumii T, Jung JC, Moskowitz MA, Fini ME, Lo EH. Effects of matrix metalloproteinase-9 gene knock-out on the proteolysis of blood-brain barrier and white matter components after cerebral ischemia. J Neurosci 2001;21:7724–32. [PubMed: 11567062]
7. Berman NE, Marcario JK, Yong C, Raghavan R, Raymond LA, Joag SV, Narayan O, Cheney PD. Microglial activation and neurological symptoms in the SIV model of NeuroAIDS: association of MHC-II and MMP-9 expression with behavioral deficits and evoked potential changes. Neurobiol Dis 1999;6:486–98. [PubMed: 10600404]
8. Bignami A, Asher R, Perides G. Co-localization of hyaluronic acid and chondroitin sulfate proteoglycan in rat cerebral cortex. Brain Res 1992;579:173–7. [PubMed: 1623404]
9. Bo L, Peterson JW, Mork S, Hoffman PA, Gallatin WM, Ransohoff RM, Trapp BD. Distribution of immunoglobulin superfamily members ICAM-1, -2, -3, and the beta 2 integrin LFA-1 in multiple sclerosis lesions. J Neuropathol Exp Neurol 1996;55:1060–72. [PubMed: 8858003]

10. Brenner DA, O'Hara M, Angel P, Chojkier M, Karin M. Prolonged activation of jun and collagenase genes by tumour necrosis factor-alpha. Nature 1989;337:661–3. [PubMed: 2537468]
11. Brightman MW, Kaya M. Permeable endothelium and the interstitial space of brain. Cell Mol Neurobiol 2000;20:111–30. [PubMed: 10696505]
12. Cardona AE, Restrepo BI, Jaramillo JM, Teale JM. Development of an animal model for neurocysticercosis: immune response in the central nervous system is characterized by a predominance of gamma delta T cells. J Immunol 1999;162:995–1002. [PubMed: 9916725]
13. Cauwe B, Van den Steen PE, Opdenakker G. The biochemical, biological, and pathological kaleidoscope of cell surface substrates processed by matrix metalloproteinases. Crit Rev Biochem Mol Biol 2007;42:113–85. [PubMed: 17562450]
14. Clark AW, Krekoski CA, Bou SS, Chapman KR, Edwards DR. Increased gelatinase A (MMP-2) and gelatinase B (MMP-9) activities in human brain after focal ischemia. Neurosci Lett 1997;238:53–6. [PubMed: 9464653]
15. Clemens JA, Stephenson DT, Smalstig EB, Dixon EP, Little SP. Global ischemia activates nuclear factor-kappa B in forebrain neurons of rats. Stroke 1997;28:1073–80. [PubMed: 9158652]discussion 1080–1
16. Corcoran ML, Stetler-Stevenson WG, Brown PD, Wahl LM. Interleukin 4 inhibition of prostaglandin E2 synthesis blocks interstitial collagenase and 92-kDa type IV collagenase/gelatinase production by human monocytes. J Biol Chem 1992;267:515–9. [PubMed: 1309751]
17. Dayer JM. How T-lymphocytes are activated and become activators by cell-cell interaction. Eur Respir J Suppl 2003;44:10s–15s. [PubMed: 14582893]
18. Ding JC, Bauer M, Diamond DM, Leal MA, Johnson D, Williams BK, Thomas AM, Najvar L, Graybill JR, Larsen RA. Effect of severity of meningitis on fungicidal activity of flucytosine combined with fluconazole in a murine model of cryptococcal meningitis. Antimicrob Agents Chemother 1997;41:1589–93. [PubMed: 9210691]
19. Elkington PT, O'Kane CM, Friedland JS. The paradox of matrix metalloproteinases in infectious disease. Clin Exp Immunol 2005;142:12–20. [PubMed: 16178851]
20. Gasche Y, Copin JC, Sugawara T, Fujimura M, Chan PH. Matrix metalloproteinase inhibition prevents oxidative stress-associated blood-brain barrier disruption after transient focal cerebral ischemia. J Cereb Blood Flow Metab 2001;21:1393–400. [PubMed: 11740200]
21. Gidday JM, Gasche YG, Copin JC, Shah AR, Perez RS, Shapiro SD, Chan PH, Park TS. Leukocyte-derived matrix metalloproteinase-9 mediates blood-brain barrier breakdown and is proinflammatory after transient focal cerebral ischemia. Am J Physiol Heart Circ Physiol 2005;289:H558–68. [PubMed: 15764676]
22. Guo P, Imanishi Y, Cackowski FC, Jarzynka MJ, Tao HQ, Nishikawa R, Hirose T, Hu B, Cheng SY. Up-regulation of angiopoietin-2, matrix metalloprotease-2, membrane type 1 metalloprotease, and laminin 5 gamma 2 correlates with the invasiveness of human glioma. Am J Pathol 2005;166:877–90. [PubMed: 15743799]
23. Gurney KJ, Estrada EY, Rosenberg GA. Blood-brain barrier disruption by stromelysin-1 facilitates neutrophil infiltration in neuroinflammation. Neurobiol Dis 2006;23:87–96. [PubMed: 16624562]
24. Jian Liu K, Rosenberg GA. Matrix metalloproteinases and free radicals in cerebral ischemia. Free Radic Biol Med 2005;39:71–80. [PubMed: 15925279]
25. Justicia C, Panes J, Sole S, Cervera A, Deulofeu R, Chamorro A, Planas AM. Neutrophil infiltration increases matrix metalloproteinase-9 in the ischemic brain after occlusion/reperfusion of the middle cerebral artery in rats. J Cereb Blood Flow Metab 2003;23:1430–40. [PubMed: 14663338]
26. Kieseier BC, Seifert T, Giovannoni G, Hartung HP. Matrix metalloproteinases in inflammatory demyelination: targets for treatment. Neurology 1999;53:20–5. [PubMed: 10408531]
27. Lacraz S, Isler P, Vey E, Welgus HG, Dayer JM. Direct contact between T lymphocytes and monocytes is a major pathway for induction of metalloproteinase expression. J Biol Chem 1994;269:22027–33. [PubMed: 8071324]
28. Leib SL, Leppert D, Clements J, Tauber MG. Matrix metalloproteinases contribute to brain damage in experimental pneumococcal meningitis. Infect Immun 2000;68:615–20. [PubMed: 10639424]

29. Leppert D, Lindberg RL, Kappos L, Leib SL. Matrix metalloproteinases: multifunctional effectors of inflammation in multiple sclerosis and bacterial meningitis. Brain Res Brain Res Rev 2001;36:249–57. [PubMed: 11690622]
30. Li Q, Park PW, Wilson CL, Parks WC. Matrilysin shedding of syndecan-1 regulates chemokine mobilization and transepithelial efflux of neutrophils in acute lung injury. Cell 2002;111:635–46. [PubMed: 12464176]
31. Maier CM, Hsieh L, Yu F, Bracci P, Chan PH. Matrix metalloproteinase-9 and myeloperoxidase expression: quantitative analysis by antigen immunohistochemistry in a model of transient focal cerebral ischemia. Stroke 2004;35:1169–74. [PubMed: 15060315]
32. McCawley LJ, Matrisian LM. Matrix metalloproteinases: multifunctional contributors to tumor progression. Mol Med Today 2000;6:149–56. [PubMed: 10740253]
33. McCoig C, Castrejon MM, Saavedra-Lozano J, Castano E, Baez C, Lanier ER, Saez-Llorens X, Ramilo O. Cerebrospinal fluid and plasma concentrations of proinflammatory mediators in human immunodeficiency virus-infected children. Pediatr Infect Dis J 2004;23:114–8. [PubMed: 14872175]
34. McQuibban GA, Gong JH, Tam EM, McCulloch CA, Clark-Lewis I, Overall CM. Inflammation dampened by gelatinase A cleavage of monocyte chemoattractant protein-3. Science 2000;289:1202–6. [PubMed: 10947989]
35. Meli DN, Loeffler JM, Baumann P, Neumann U, Buhl T, Leppert D, Leib SL. In pneumococcal meningitis a novel water-soluble inhibitor of matrix metalloproteinases and TNF-alpha converting enzyme attenuates seizures and injury of the cerebral cortex. J Neuroimmunol 2004;151:6–11. [PubMed: 15145598]
36. Mertz PM, DeWitt DL, Stetler-Stevenson WG, Wahl LM. Interleukin 10 suppression of monocyte prostaglandin H synthase-2. Mechanism of inhibition of prostaglandin-dependent matrix metalloproteinase production. J Biol Chem 1994;269:21322–9. [PubMed: 8063757]
37. Miltenburg AM, Lacraz S, Welgus HG, Dayer JM. Immobilized anti-CD3 antibody activates T cell clones to induce the production of interstitial collagenase, but not tissue inhibitor of metalloproteinases, in monocytic THP-1 cells and dermal fibroblasts. J Immunol 1995;154:2655–67. [PubMed: 7876539]
38. Nag S, Picard P, Stewart DJ. Expression of nitric oxide synthases and nitrotyrosine during blood-brain barrier breakdown and repair after cold injury. Lab Invest 2001;81:4–9.
39. Nourhaghighi N, Teichert-Kuliszewska K, Davis J, Stewart DJ, Nag S. Altered expression of angiopoietins during blood-brain barrier breakdown and angiogenesis. Lab Invest 2003;83:1211–22. [PubMed: 12920250]
40. Nygardas PT, Hinkkanen AE. Up-regulation of MMP-8 and MMP-9 activity in the BALB/c mouse spinal cord correlates with the severity of experimental autoimmune encephalomyelitis. Clin Exp Immunol 2002;128:245–54. [PubMed: 11985514]
41. Piccio L, Rossi B, Scarpini E, Laudanna C, Giagulli C, Issekutz AC, Vestweber D, Butcher EC, Constantin G. Molecular mechanisms involved in lymphocyte recruitment in inflamed brain microvessels: critical roles for P-selectin glycoprotein ligand-1 and heterotrimeric G(i)-linked receptors. J Immunol 2002;168:1940–9. [PubMed: 11823530]
42. Rascher G, Fischmann A, Kroger S, Duffner F, Grote EH, Wolburg H. Extracellular matrix and the blood-brain barrier in glioblastoma multiforme: spatial segregation of tenascin and agrin. Acta Neuropathol (Berl) 2002;104:85–91. [PubMed: 12070669]
43. Rosenberg GA. Matrix metalloproteinases and neuroinflammation in multiple sclerosis. Neuroscientist 2002;8:586–95. [PubMed: 12467380]
44. Rosenberg GA, Mun-Bryce S. Matrix metalloproteinases in neuroinflammation and cerebral ischemia. Ernst Schering Res Found Workshop 2004:1–16. [PubMed: 15032051]
45. Rosenberg GA, Sullivan N, Esiri MM. White matter damage is associated with matrix metalloproteinases in vascular dementia. Stroke 2001;32:1162–8. [PubMed: 11340226]
46. Sellebjerg F, Sorensen TL. Chemokines and matrix metalloproteinase-9 in leukocyte recruitment to the central nervous system. Brain Res Bull 2003;61:347–55. [PubMed: 12909304]
47. Sellner J, Leib SL. In bacterial meningitis cortical brain damage is associated with changes in parenchymal MMP-9/TIMP-1 ratio and increased collagen type IV degradation. Neurobiol Dis 2006;21:647–56. [PubMed: 16257222]

48. Shapiro S, Miller A, Lahat N, Sobel E, Lerner A. Expression of matrix metalloproteinases, sICAM-1 and IL-8 in CSF from children with meningitis. J Neurol Sci 2003;206:43–8. [PubMed: 12480084]
49. Sixt M, Engelhardt B, Pausch F, Hallmann R, Wendler O, Sorokin LM. Endothelial cell laminin isoforms, laminins 8 and 10, play decisive roles in T cell recruitment across the blood-brain barrier in experimental autoimmune encephalomyelitis. J Cell Biol 2001;153:933–46. [PubMed: 11381080]
50. Strazielle N, Khuth ST, Murat A, Chalon A, Giraudon P, Belin MF, Ghersi-Egea JF. Pro-inflammatory cytokines modulate matrix metalloproteinase secretion and organic anion transport at the blood-cerebrospinal fluid barrier. J Neuropathol Exp Neurol 2003;62:1254–64. [PubMed: 14692701]
51. Sugita S, Saito F, Tang J, Satz J, Campbell K, Sudhof TC. A stoichiometric complex of neurexins and dystroglycan in brain. J Cell Biol 2001;154:435–45. [PubMed: 11470830]
52. Talts JF, Andac Z, Gohring W, Brancaccio A, Timpl R. Binding of the G domains of laminin alpha1 and alpha2 chains and perlecan to heparin, sulfatides, alpha-dystroglycan and several extracellular matrix proteins. Embo J 1999;18:863–70. [PubMed: 10022829]
53. Tian M, Jacobson C, Gee SH, Campbell KP, Carbonetto S, Jucker M. Dystroglycan in the cerebellum is a laminin alpha 2-chain binding protein at the glial-vascular interface and is expressed in Purkinje cells. Eur J Neurosci 1996;8:2739–47. [PubMed: 8996823]
54. Toft-Hansen H, Nuttall RK, Edwards DR, Owens T. Key metalloproteinases are expressed by specific cell types in experimental autoimmune encephalomyelitis. J Immunol 2004;173:5209–18. [PubMed: 15470066]
55. Tseng YK, Tu WC, Lee HH, Chen KM, Chou HL, Lai SC. Ultrastructural localization of matrix metalloproteinase-9 in eosinophils from the cerebrospinal fluid of mice with eosinophilic meningitis caused by Angiostrongylus cantonensis. Ann Trop Med Parasitol 2004;98:831–41. [PubMed: 15667715]
56. Unemori EN, Hibbs MS, Amento EP. Constitutive expression of a 92-kD gelatinase (type V collagenase) by rheumatoid synovial fibroblasts and its induction in normal human fibroblasts by inflammatory cytokines. J Clin Invest 1991;88:1656–62. [PubMed: 1658048]
57. van Horssen J, Bo L, Vos CM, Virtanen I, de Vries HE. Basement membrane proteins in multiple sclerosis-associated inflammatory cuffs: potential role in influx and transport of leukocytes. J Neuropathol Exp Neurol 2005;64:722–9. [PubMed: 16106221]
58. Vecil GG, Larsen PH, Corley SM, Herx LM, Besson A, Goodyer CG, Yong VW. Interleukin-1 is a key regulator of matrix metalloproteinase-9 expression in human neurons in culture and following mouse brain trauma in vivo. J Neurosci Res 2000;61:212–24. [PubMed: 10878594]
59. Vos CM, van Haastert ES, de Groot CJ, van der Valk P, de Vries HE. Matrix metalloproteinase-12 is expressed in phagocytotic macrophages in active multiple sclerosis lesions. J Neuroimmunol 2003;138:106–14. [PubMed: 12742660]
60. Wahl LM, Corcoran ME, Mergenhagen SE, Finbloom DS. Inhibition of phospholipase activity in human monocytes by IFN-gamma blocks endogenous prostaglandin E2-dependent collagenase production. J Immunol 1990;144:3518–22. [PubMed: 2158512]
61. White AC Jr, Robinson P, Kuhn R. Taenia solium cysticercosis: host-parasite interactions and the immune response. Chem Immunol 1997;66:209–30. [PubMed: 9103671]
62. Yang Y, Estrada EY, Thompson JF, Liu W, Rosenberg GA. Matrix metalloproteinase-mediated disruption of tight junction proteins in cerebral vessels is reversed by synthetic matrix metalloproteinase inhibitor in focal ischemia in rat. J Cereb Blood Flow Metab 2007;27:697–709. [PubMed: 16850029]
63. Yong VW, Power C, Forsyth P, Edwards DR. Metalloproteinases in biology and pathology of the nervous system. Nat Rev Neurosci 2001;2:502–11. [PubMed: 11433375]
64. Zaccaria ML, Di Tommaso F, Brancaccio A, Paggi P, Petrucci TC. Dystroglycan distribution in adult mouse brain: a light and electron microscopy study. Neuroscience 2001;104:311–24. [PubMed: 11377836]

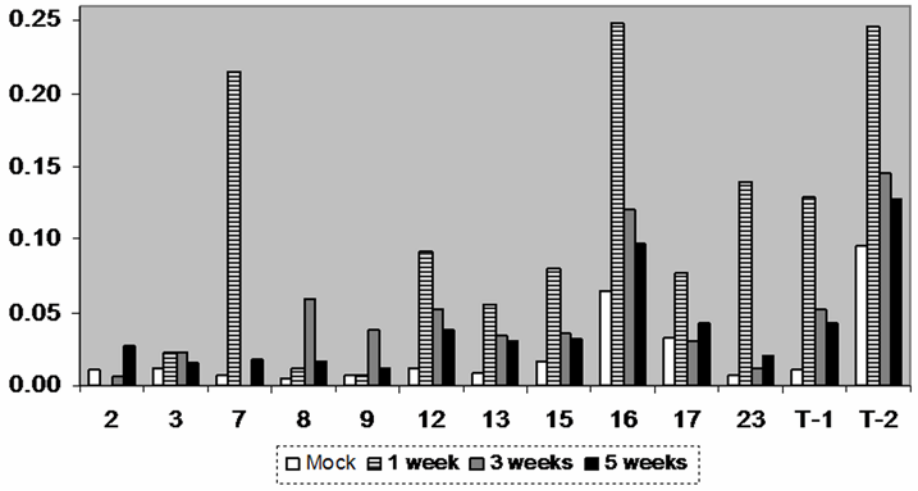

Figure 1. MMP expression is upregulated during the course of murine NCC

Total RNA was isolated from mock and infected controls at different post infection times. After reverse transcription in presence of α-^{33}P-dCTP, the cDNA probes were hybridized to GEArray Q series membranes. The levels of mRNA expression of distinct MMPs were calculated in arbitrary units and normalized to the average of housekeeping genes. Normalized values are shown in the y-axis and represent the mean of two independent experiments. MMPs are denoted by their number. T-1 and T-2 represent TIMP-1 and TIMP-2 respectively.

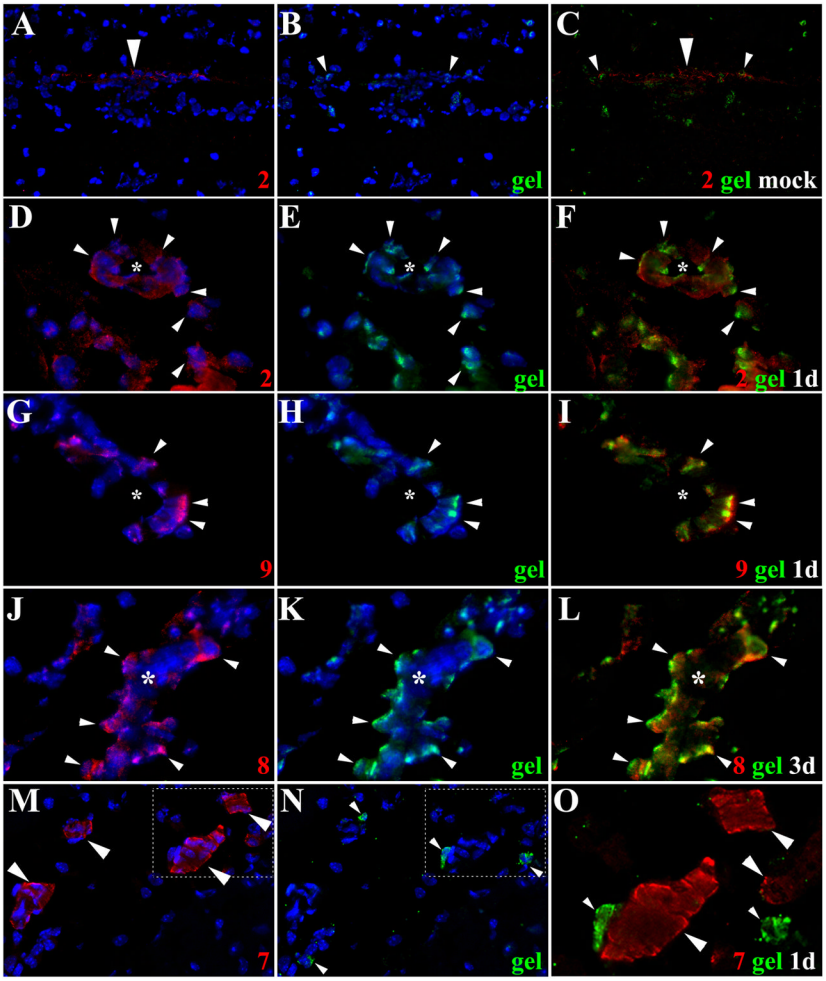

Figure 2. Extravasation of leukocytes through pial vessels involves expression of active MMPs early in the infectious process

ISZ and IF were performed in mock and animals infected with *M. corti* for 1 (1d) and 3 days (3d). MMPs are labeled red (Rhodamine red X) and their activity, detected as gelatin (**gel**) degradation appears green (fluorescein). Nuclear staining (DAPI) is blue. Three images (MMP +DAPI)-(gel+DAPI)-(MMP+gel) of the same field were included for clarity. **(A)** Low expression of MMP-2 in pial vessel (large arrowhead) of mock infected animal. 40X **(B)** Active gelatinolysis in leukocytes (arrowheads) located in vicinity of pial vessel **(C)** Modest expression of active MMP-2 in leukocytes (small arrowheads) extravasating pial vessel (large arrowhead) **(D)** MMP-2 expression in pial vessel (asterisk) and infiltrating cells (arrowheads). 1d - 100X **(E)** Gelatinolytic activity in cells (arrowheads) traversing pial vessel (asterisk) **(F)** Gelatinolysis and MMP-2 expression in cells (arrowheads) extravasating pial vessel (asterisk) and accumulating in perivascular areas **(G)** Extravasating cells (arrowheads) showing polarized MMP-9 expression from the lumen towards the basal lamina in a pial vessel (asterisk). 1d – 100X **(H)** Polarized gelatinolysis in cells (arrowheads) traversing pial vessel (asterisk) **(I)** Active MMP-9 expression in cells (arrowheads) infiltrating into the CNS through a pial vessel (asterisk) **(J)** Extravasating cells (arrowheads) displaying polarized MMP-8 expression from the lumen towards the basal lamina in pial vessel (asterisk). 3d – 100X **(K)** Polarized gelatinolysis in cells (arrowheads) traversing pial vessel (asterisk) **(L)** Active MMP-8 expression in cells (arrowheads) traversing a pial vessel (asterisk) **(M)** Expression of MMP-7 in pial vessels (arrowheads). 1d - 63X **(N)** Infiltrating leukocytes (arrowheads) displaying

gelatinolysis **(O)** High power view of area marked in M and N, showing lack of gelatinolysis in MMP-7 positive pial vessels (large arrowheads), and high expression in basal lamina. Gelatin degradation is seen in MMP-7 negative leukocytes (small arrowheads).

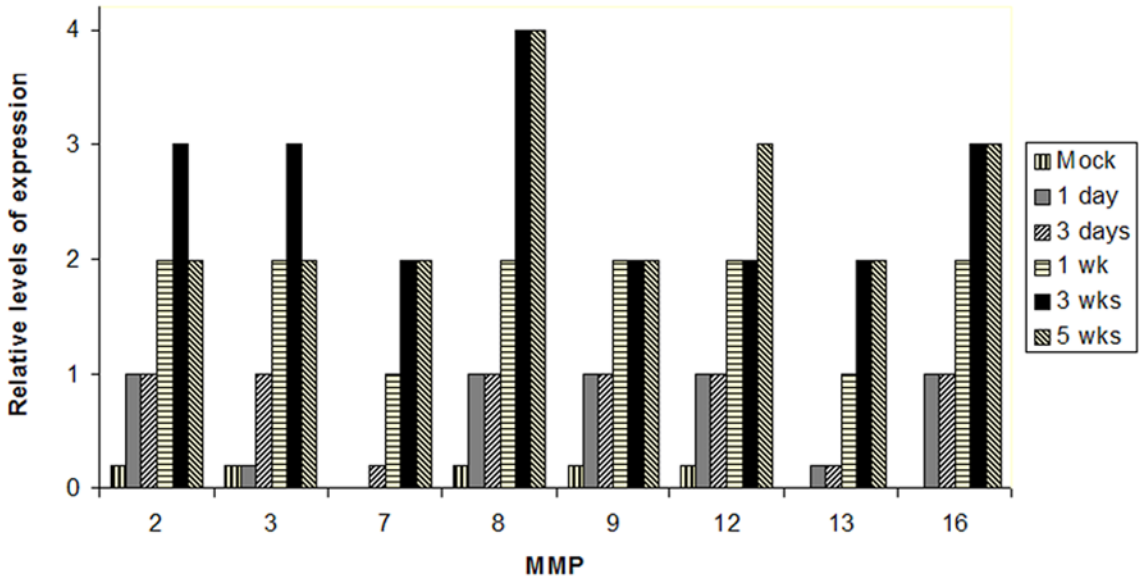

Figure 3. Kinetics and relative levels of MMP expression in leukocytes extravasating and infiltrating the CNS during the course of murine NCC

Mice were intracranially inoculated with *M. corti* and sacrificed at the indicated times. 3 animals were analyzed per each infection time. MMPs (x axis) were determined using the polyclonal antibodies described in material and methods. The relative number of cells at each post infection time was arbitrarily assigned a number from 0 to 4 representing absent to abundant.

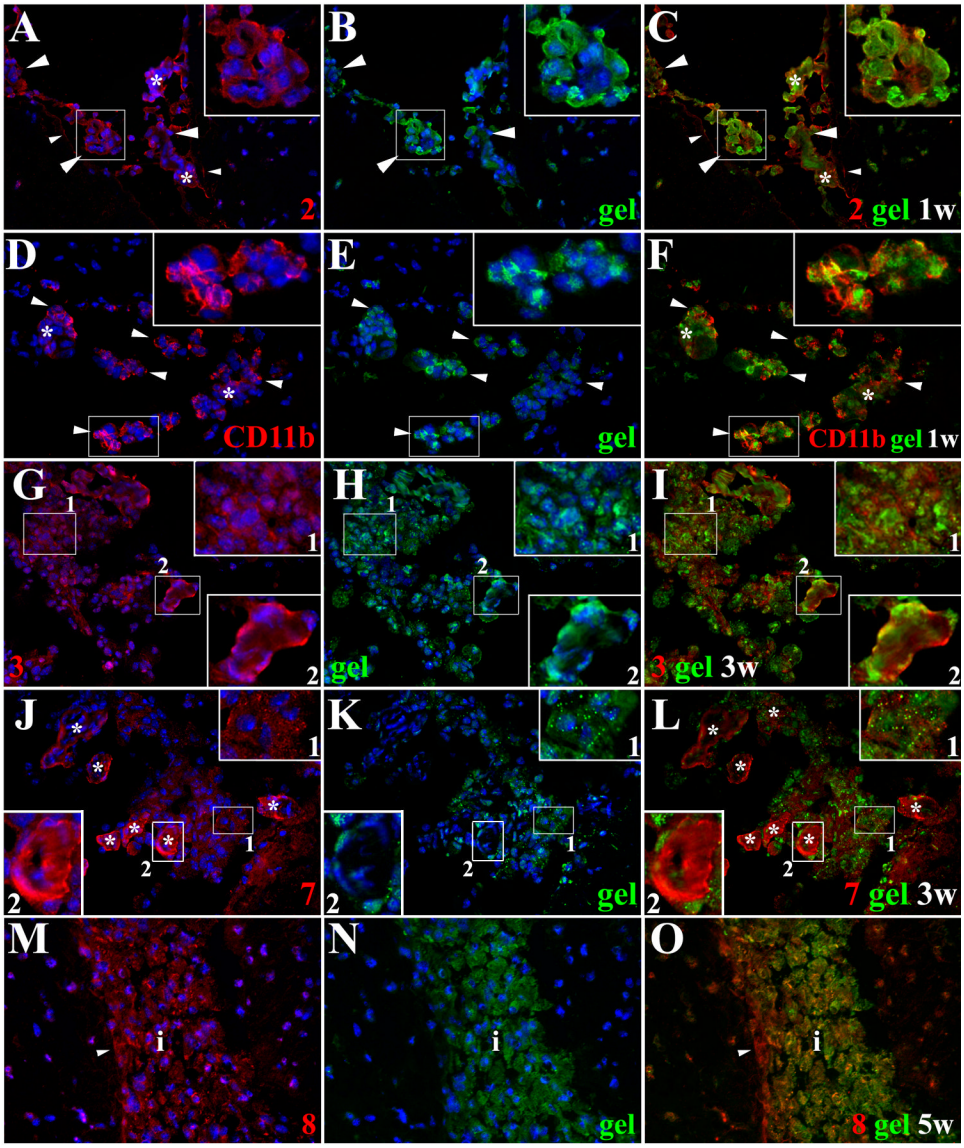

Figure 4. Expression of active MMPs detected by gelatin cleavage in leptomeningeal infiltrates during the course of murine NCC

ISZ detected as **gel** (green) degradation and MMP expression (red) were performed in *M. corti* infected animals 1 (1w), 3 (3w) and 5 weeks (5w) post-infection. Nuclear staining (DAPI) is blue. Three images (MMP+DAPI)-(gel+DAPI)-(MMP+gel) of the same field were included for clarity. High power view insets (2.5X times magnified) of pictures A to L were added to better illustrate MMP activity. **(A)** MMP-2 expression in leukocytes extravasating pial vessels (asterisks) and infiltrating leptomeninges (large arrowheads). Astrocyte endfeet processes (small arrowheads) also express MMP-2. 1w - 40X **(B)** Same field as A showing gelatinolysis **(C)** Cells extravasating pial vessels (asterisks) and infiltrating leptomeninges (large arrowheads) express active MMP-2. Astrocyte endfeet (small arrowheads) also express MMP-2, but lack gelatinolysis **(D)** CD11b+ leukocytes extravasating pial vessels (asterisks) and accumulating in internal leptomeninges (arrowheads). 1w - 40X **(E)** same field as D showing gelatin degradation **(F)** CD11b+ infiltrates (arrowheads) actively degrading gelatin **(G)** MMP-3 expression in leukocytes infiltrating internal leptomeninges (inset 1) and pial vessels (inset 2). 3w - 40X **(H)** same field as G showing gelatin degradation **(I)** Infiltrates (inset

1) in internal leptomeninges express active MMP-3, gelatin degradation is also detected in pial vessels (inset 2) **(J)** Infiltrating leukocytes (inset 1) and pial vessels (asterisks - inset 2) in internal leptomeninges expressing MMP-7. 3w - 40X **(K)** same field as J showing gelatin degradation **(L)** Active MMP-7 is moderately expressed in infiltrating cells (inset 1). Low gelatin degradation is detected in pial vessels (asterisks - inset 2) **(M)** High expression of MMP-8 in leptomeningeal infiltrate (i). Astrocyte endfeet (small arrowhead) opposed to the pia also express MMP-8. 5w - 40X **(N)** same field as M showing gelatinolysis **(O)** Active expression of MMP-8 in leptomeningeal infiltrate (i). Astrocyte endfeet lack gelatin degradation.

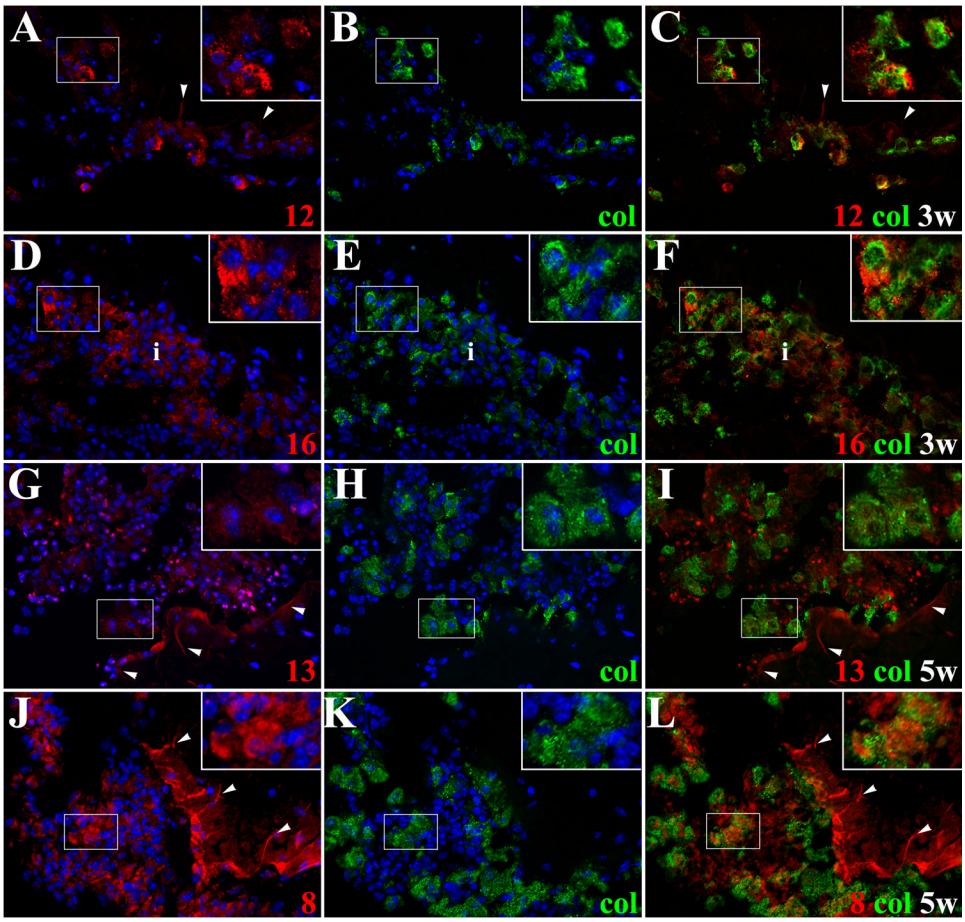

Figure 5. Active MMPs detected by collagen cleavage are present in inflammatory infiltrates of mice infected with *M. corti*

ISZ using collagen (**col**)-oregon 488 (green) as substrate and MMP expression (red) were performed in *M. corti* infected animals 1w, 3w and 5w post-infection. Nuclear staining (DAPI) is blue. Three images (MMP+DAPI)-(col+DAPI)-(MMP+col) of the same field were included for clarity. High power view insets (2.5X times magnified) were added to better illustrate MMP activity **(A)** MMP-12 expressed by leukocytes infiltrating (inset) external leptomeninges and by astrocyte endfeet (arrowheads). 1w - 40X **(B)** Same field as A, but showing collagenolysis **(C)** Collagen cleavage is detected in MMP-12 expressing leukocytes (inset), but no in astrocyte endfeet (arrowheads) **(D)** Leukocytes in inflammatory infiltrates (i) at internal leptomeninges expressing MMP16. 3w - 40X **(E)** Same field as D showing collagenolysis **(F)** Leukocytes (i) infiltrating internal leptomeninges express active MMP-16 **(G)** MMP-13 expression in internal leptomeninges infiltrates (inset) and astrocyte endfeet (arrowheads). 5w - 40X **(H)** same field as G, but showing collagen cleavage **(I)** Active MMP-13 is modestly expressed by some cells in inflammatory infiltrates (inset), inactive MMP-13 is detected in astrocyte endfeet (arrowheads) **(J)** High expression of MMP-8 in internal leptomeninges infiltrates (inset) and astrocyte endfeet (arrowheads). 5w - 40X **(K)** Same field as J, showing collagenolysis **(L)** Active expression of MMP-8 in leptomeningeal infiltrates (inset), inactive enzyme is detected in few inflammatory cells and astrocyte endfeet (arrowheads).

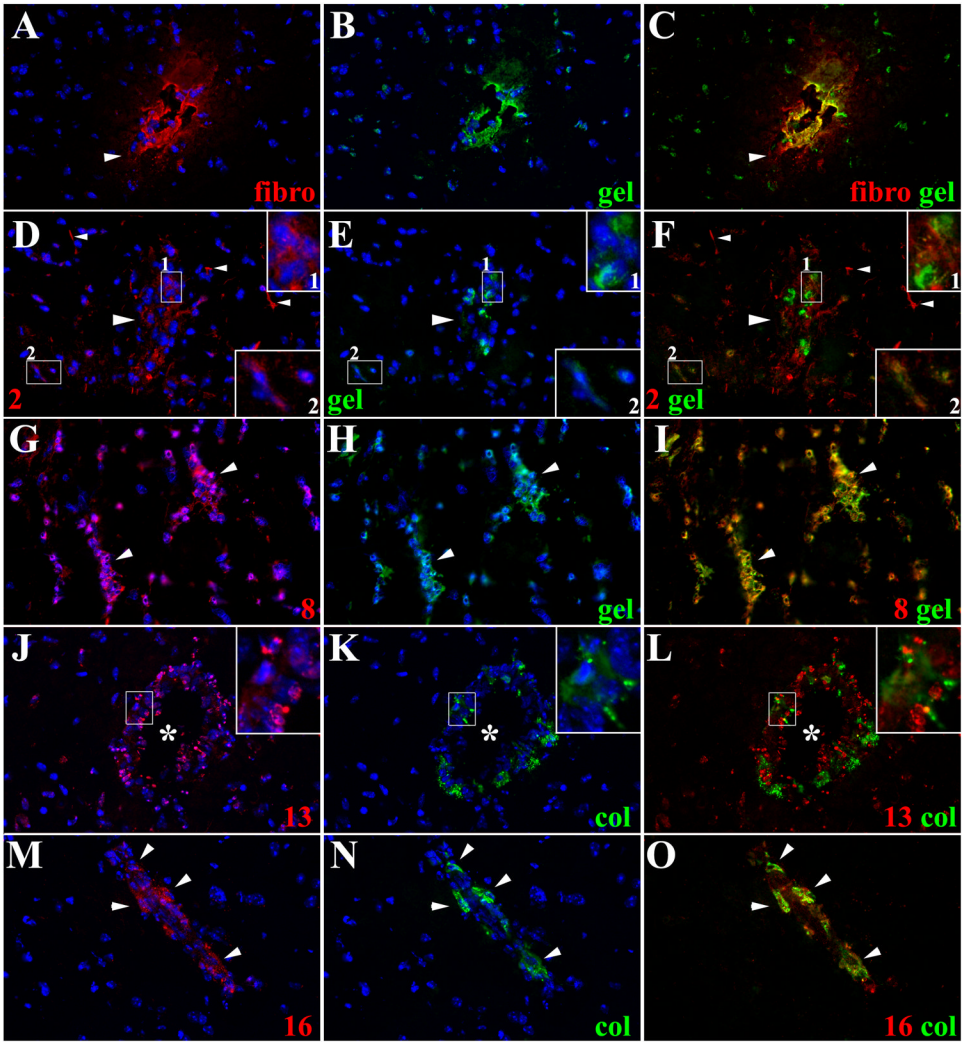

Figure 6. Expression of active MMPs in leukocytes infiltrating CNS parenchyma

ISZ using **gel** and **col**(green) combine with IF detection of MMPs (red) were used to determine the expression of active MMPs in leukocytes extravasating parenchymal vessels 5w post-infection. Nuclear staining is blue. Three images (MMP+DAPI)-(gel+DAPI)-(MMP+gel) of the same field were included for clarity. High power view insets (2.5X times magnified) of pictures D to F and J to L were added to better illustrate MMP activity **(A)** Fibronectin extravasation (arrowhead) in parenchymal vessel. 40X **(B)** same field as A showing gelatin degradation **(C)** Active gelatinolysis in parenchymal vessel displaying fibronectin extravasation **(D)** MMP-2 expression in leukocytes extravasating parenchymal vessel (large arrowhead - inset 1), microglia-astrocyte like cells (inset 2) and astrocyte endfeet (small arrowheads). 40X **(E)** same field as D showing gelatin degradation **(F)** Active MMP-2 expression in some of the leukocytes extravasating a parenchymal vessel (large arrowhead-inset 1) and in microglia-astrocyte like cells (inset 2). MMP-2 expressed in astrocyte endfeet (small arrowheads) does not cleave gelatin **(G)** Expression of MMP-8 in leukocytes extravasating parenchymal vessels (arrowheads). 40X **(H)** same field as G showing gelatin degradation **(I)** Active MMP-8 expression by leukocytes in perivascular infiltrates of parenchymal vessels (arrowheads) **(J)** Leukocytes extravasating parenchymal vessel (asterisk) displayed moderate MMP-13 expression (inset). 40X **(K)** Same field as J showing collagen degradation **(L)** Active collagen degradation is detected in few MMP-13 positive leukocytes

(inset) extravasating a parenchymal vessel (asterisk) **(M)** MMP-16 expression in leukocytes (arrowheads) extravasating a parenchymal vessel. 40X **(N)** same field as M showing collagenolysis **(O)** Active expression of MMP-16 in leukocytes extravasating a parenchymal vessel.

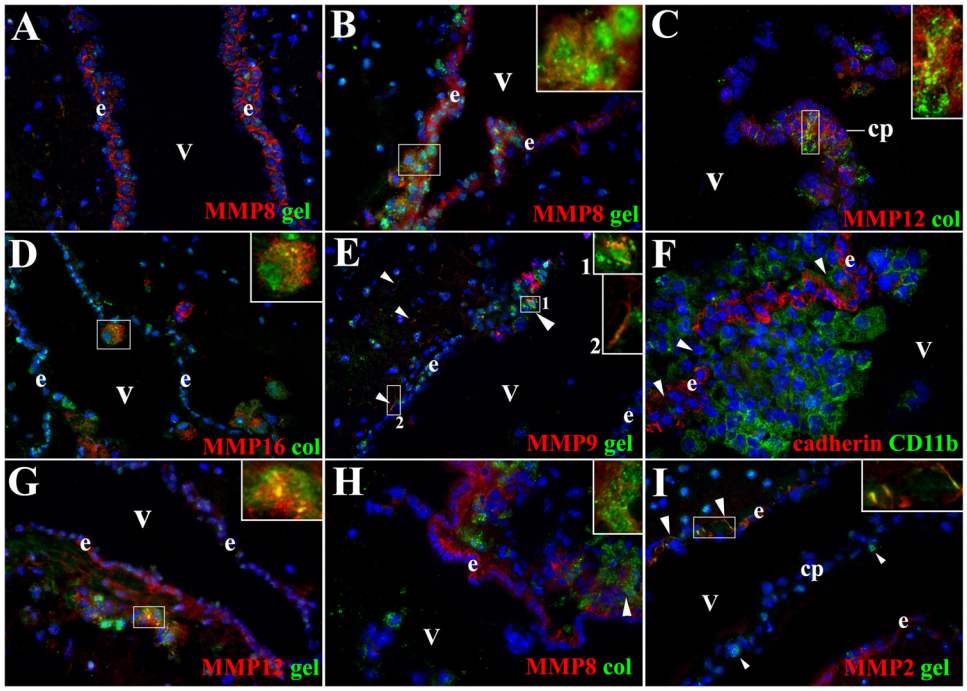

Figure 7. MMP expression in ependyma, CP and leukocytes infiltrating ventricle in mice infected with *M. corti*

ISZ with **gel** and **col** (green) as substrates and IF with polyclonal antibodies against distinct MMPs (red) were used to determine the expression of active MMPs in ventricular areas during infection. Panel D shows cadherin expression (red) and $CD11b^+$ cells (green). High power view insets (2.5X times magnified) were included in some pictures to better illustrate MMP activity. Nuclear staining is blue. Ventricle (**v**), ependyma (**e**) and choroid plexus (**cp**). **(A)** MMP-8 expression and low gelatinolysis is detected in **e** of mock infected animal. 40X **(B)** MMP-8 expression increased in **e**. Active and polarized expression of this enzyme was found in leukocytes (inset) traversing this structure. 1w 40X **(C)** MMP-12 expression was detected in **cp** and leukocytes (inset) migrating into the **v**, active enzyme was only detected in leukocytes (inset). 1w 40X **(D)** Active MMP-16 expressed in leukocytes (inset) migrating through **e** into **v**. 1w - 40X **(E)** Expression of active MMP-9 in cells (large arrowhead – inset 1) moving from subependyma into ventricles. Subependymal astrocyte endfeet (small arrowheads – inset 2) also express MMP-9 able to degrade gelatin. 1w - 40X **(F)** High infiltration of $CD11b^+$ cells into ventricle through holes (arrowheads) in the **e** labeled with pan-cadherin antibody. 3w - 63X **(G)** Active gelatinolysis by MMP-12 was detected in leukocytes (arrowheads - inset) located under **e**. Moderate upregulation of inactive MMP-12 was detected in **e**. 3w - 40X **(H)** Active MMP-8 expression in leukocytes (arrowhead – inset) located under **e**. Moderate upregulation of inactive MMP-8 is detected in **e**. 3w - 40X **(I)** Subependymal astrocyte endfeet (large arrowheads - inset) expressed MMP-2 displaying gelatinolytic activity. No MMP-2 expression was detected in **cp** or in cells extravasating the **cp** (small arrowheads). 3w - 40X

Table 1

Enzymatic activity of MMPs in murine NCC[a]

	Mock	1 day	3 days	1 wk	3 wks	5 wks	Level of MMP expression[b]
Gelatin							
Mononuclear cells[c]	+/–[d]	+	+	++	+++	++	8, 16, 3, 9, 2, 12, 13, 7
Pial vessels	-	+/–	+	+	++	+	3, 7, 2, 8, 16, 9
Astrocytes[e]	-	-	-	+/–	+	++	2, 8, 9, 3, 12, 13, 16
Ependyma	-	+/–	+/–	+	++	+	8, 3, 12, 2, 9, 16
Ch plexus	-	-	-	+/–	+/–	+/–	3, 12, 8
Collagen							
Mononuclear cells[c]	-	+/–	+	+	++	+++	8, 16, 12, 3, 13, 9, 2

[a] Mice were intracranially inoculated with *M. corti* and sacrificed at the indicated times. 3 animals were analyzed per each infection time.

[b] MMPs were determined using the polyclonal antibodies described in material and methods. Level of expression reads from maximum (left) to minimum (right).

[c] MMP activity was determined by ISZ utilizing DQ-gelatin and collagen (col) highly quenched with fluorescein and oregon 488 respectively. Gelatinolysis was detected in all the cells/areas studied whereas collagenolysis was only found in mononuclear cells.

[d] The relative enzymatic activity at each post infection time was arbitrarily assigned and represent: - (absent) to +++ (abundant).

[e] Astrocyte endfeet located in the subependyma displayed moderate gelatinolytic activity